ELSEVIER

Journal of Nuclear Materials 241–243 (1997) 433–437

journal of nuclear materials

Assessment of the DIVIMP 'onion-skin' model in the JET Mark I divertor

S.K. Erents [b,*], P. Breger [a], S.J. Davies [a], J.D. Elder [c], H.Y. Guo [d], L.D. Horton [a], G.F. Matthews [a], R.D. Monk [a], P.C. Stangeby [c], D.D.R. Summers [a]

[a] *JET Joint Undertaking, Abingdon, Oxon OX14 3EA, UK*
[b] *UKAEA Culham Laboratory, Abingdon, Oxon OX14 3DB, UK*
[c] *Institute for Aerospace Studies, University of Toronto, Downsview, Ont., Canada M3H 5T6*
[d] *INRS-Energie et Materiaux, University du Quebec, Quebec, Canada*

Abstract

The DIVIMP-NIMBUS [1] 'Onion-Skin' model has been used to predict upstream plasma parameters using as input measurements by Langmuir probes in the divertor target tiles. Measurements of density and temperature (both T_i and T_e) across the SOL close to the stagnation point at the top of the torus have been made using a reciprocating probe carrying both Langmuir and retarding field analyzer (RFA) heads. In addition, a lithium beam diagnostic has been used to measure radial distributions of density upstream. Ohmic, L-mode and H-mode discharges have been studied, and good agreement with code predictions in the three cases has been found. The heat transport coefficient, $\chi_\perp(r)$, has been evaluated across the SOL, and is found to increase with increasing distance from the separatrix.

Keywords: JET; Divertor plasma; 2D model; Monte Carlo simulation; Transverse transport

1. Introduction

DIVIMP (divertor impurity) is a Monte Carlo code [1] which follows impurity particles in a hydrogenic background plasma calculated, for example, by an 'onion-skin' (O-S) model. It is important to establish that this background plasma is itself correct before proceeding with impurity modelling. The objective of the present work is to validate the DIVIMP-NIMBUS O-S, (D-N O-S) model for ohmic, L-mode and H-mode plasmas. This is achieved here using Langmuir probe data from probes in the divertor target tiles as input to the D-N O-S code, and comparing the code predictions upstream with experimental measurements from Langmuir, retarding field analyzer (RFA), and lithium beam probes.

In contrast to most fluid codes, for example EDGE2D/NIMBUS used at JET [2] and B2/EIRENE as used at Culham and other laboratories [3], the D-N O-S code uses *target* experimental measurements to define the boundary conditions at the divertor target. A series of 1D fluid equations are then solved along the magnetic flux tubes connecting the target with the upstream SOL, assuming that plasma transport is dominated by parallel flow of particles and heat. In the model, ion and electron heat transport are treated separately. The fluid equations are solved for a number of flux tubes at different radii, which then result in a 2D, O-S representation of the entire SOL.

An important feature of the D-N O-S code is the inclusion of recycled neutral hydrogen particles and their ionization. To achieve this, the D-N O-S code repeatedly calls the 2D hydrogenic ionization code NIMBUS [4], and iterates with the ionization pattern which is produced until a convergence is obtained. Radiative cooling can be allowed for, according to an analytic prescription for both its magnitude and spacial distribution. The model also uses conservation of momentum and energy along the field lines.

Having validated the D-N O-S code using experimental measurements of upstream density n_{eu}, and electron and

* Corresponding author. Tel.: +44-1235 46 3438; fax: +44-1235 46 4192.

PII S0022-3115(96)00542-9

ion temperatures T_{eu} and T_{iu}, it is then possible to use the radial distributions of these parameters in the SOL to calculate the transport coefficients. Unfortunately, for the present case, the ionization in the SOL is much less than the flow across the separatrix by cross-field diffusion. This makes the calculation of $D_\perp(r)$ subject to large error. This is not the case for $\chi_\perp(r)$, however, since there is virtually no heat source within the SOL. The D-N O-S code contains an 'extractor' for calculating $\chi_\perp(r)$, an extension [5] of that described in Ref. [6].

2. Code assumptions

The D-N O-S code produces a 2D distribution of n_e, T_i and T_e, parallel plasma drift velocity v_b and parallel electric field $E_\parallel$. Here we use DIVIMP's 'SOL option 22' which uses a Runge Kutta method to solve the SOL equations which include parallel convection.

The present D-N O-S code assumes:

– Parallel pressure balance,

$$2 \cdot n_{et}(T_{et} + T_{it}) = n_{eu}(T_{eu} + T_{iu}) = n_e(T_e + T_i + m_i v^2) \tag{1}$$

(where suffixes t and u refer to target and upstream). Neutral friction is neglected in this version of the O-S code.

– Parallel heat conduction,

$$q_\parallel^{e,i}, \text{cond} \approx -\kappa_{0e,i} T_{e,i}^{5/2} \frac{dT_{e,i}}{ds} \tag{2}$$

– Parallel heat convection:

$$q_\parallel^{e,i}, \text{conv} = \left(\tfrac{5}{2} k T_{e,i} + \tfrac{1}{2} m_{e,i} v^2\right) nv \tag{3}$$

– Electron and ion particle and heat balance are treated separately, giving

$$T_e \neq T_i, \tag{4}$$

generally.

– $T_{it} = T_{et}$ is assumed for the discharges considered here, (exceptionally),

$$T_{it} = 2 \cdot T_{et} \tag{5}$$

Volumetric power loss/gain associated with recycling is neglected in this version of the O-S code.

– mach number = unity at the target (6)

– Recombination is neglected in this version of the O-S code. A fuller version of the D-N O-S code is described in Ref. [5].

3. Experimental measurements

An array of probes in the divertor target tiles recorded ion saturation current, j_{sat} (A m^{-2}) and T_{et} which were used as input for the D-N O-S code. T_{it} is also required as a code input, and usually $T_{it} = T_{et}$ was assumed. Radial profiles of these parameters across the tiles were measured by sweeping the separatrix location across the probes at 4 Hz. For all discharges recorded here, the separatrix location remained on the lower target tiles during the sweep. No discharges were close to divertor detachment.

Three diagnostics were used to measure radial profiles of upstream plasma parameters near to the stagnation point at the top of the torus. The Langmuir probes and RFA were carried on a reciprocating probe, (located at $R = 3.25$ m), which moves 100 mm in and out of the plasma in a time of 400 ms. The probes typically just reach the separatrix position, although in some discharges have moved some 20 mm inside the separatrix. The single Langmuir probes make a complete I/V ($-200 < V < 20$ V) scan typically every 10 ms. The standard deviations in the fitting of the Langmuir characteristics are usually much less than the real fluctuations in T_e between one time point and the next. Most probes sample the plasma from the ion drift direction, connecting to the outer divertor target, with the exception of the RFA probe which samples the electron drift direction.

To record $T_i(r)$, an RFA is used with a 30 μm slit on the ion drift side of the probe, i.e. facing towards the outer divertor target along the field lines. The RFA I/V characteristics show the ion distribution function to be a shifted Maxwellian, with a sheath potential close to 100 V near to the separatrix. A single Langmuir probe records $T_e(r)$ simultaneously.

In high power H-mode plasmas it is dangerous to use the reciprocating probe very close to the separatrix because a disruption may result in very high power deposition and breakage of the carbon body of the probe. For the next campaign, a insulating boron nitride body is to be used which should minimize $J \times B$ forces. Therefore, for H-mode plasmas upstream density was measured using a lithium beam diagnostic [7]. The lithium beam is located at the top of the torus very close (radially) to the reciprocating probe position.

4. Results

4.1. Code input data

Upstream measurements of $n_e(r)$, $T_e(r)$ and $T_i(r)$ have been made for a variety of ohmic, L-mode and H-mode discharges. Target probe measurements have been made for most discharges (but not all with separatrix scanning). In some discharges, measurements are limited to those from triple probes, rather than single Langmuir probes. Examples of the input data used by D-N O-S for $j_{sat}(r)$ and $T_e(r)$ are shown in Figs. 1 and 2. For each 'ring' intersecting the target tiles, the average j_{sat} and T_{et} in the fluctuating plasma is used.

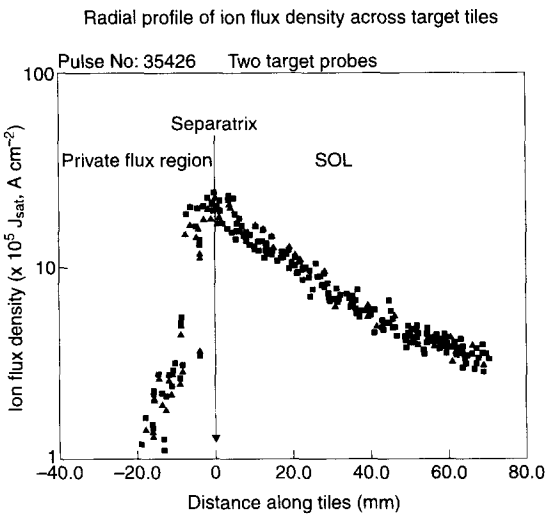

Fig. 1. Radial profile of J_{sat} across target tiles, used as input for the D-N O-S code.

4.2. Comparison of experimental upstream data with code predictions

4.2.1. Ohmic

$I_p = 2$ MA, $B_T = 2.9$ T, $\overline{n_e} = 2.7 \times 10^{19}$ m^{-3}.

In Figs. 3 and 4, the upstream T_{eu} and n_{eu} were measured using the single Langmuir reciprocating probe, which for this discharge moved just inside the separatrix (confirmed by pressure balance). There is considerable fluctuation in the experimental data, but the code simulation is good.

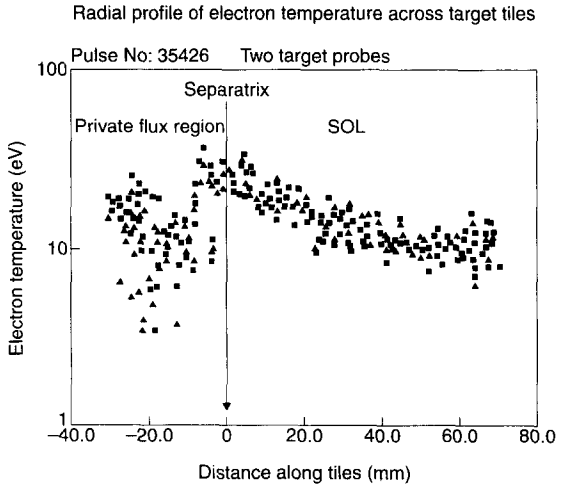

Fig. 2. Radial profile of T_e across target tiles, used as input for the D-N O-S code.

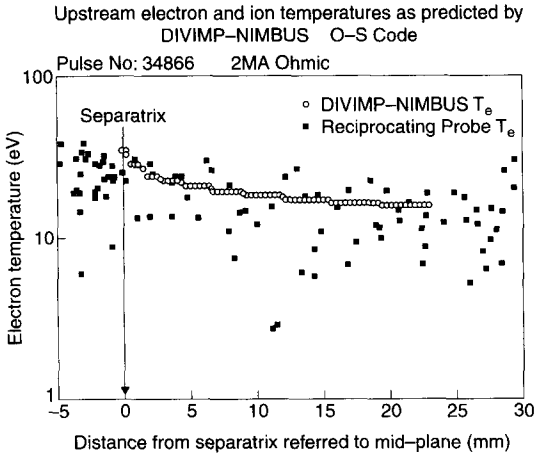

Fig. 3. D-N O-S code simulation of a 2 MA ohmic discharge, upstream data provided by a single Langmuir probe.

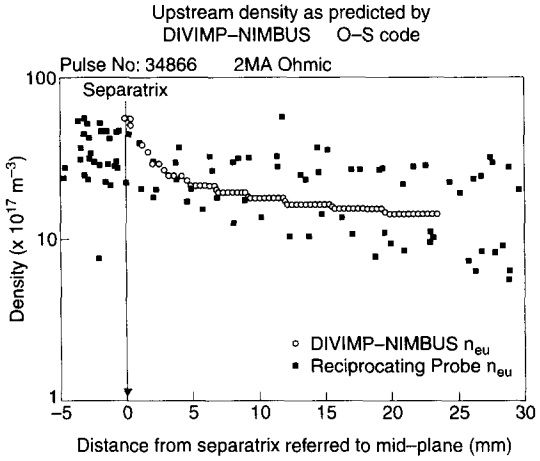

Fig. 4. D-N O-S code simulation of a 2 MA ohmic discharge, upstream data provided by a single Langmuir probe.

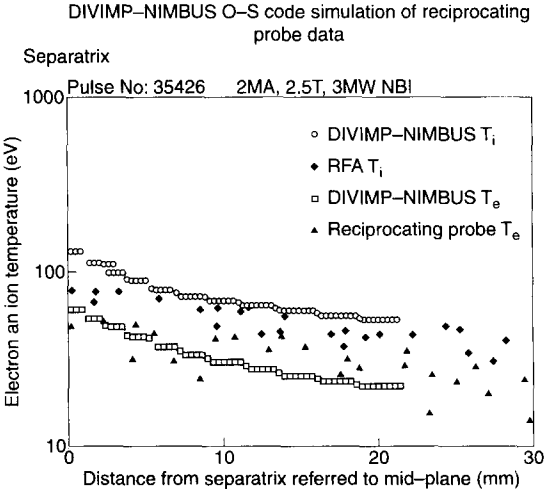

Fig. 5. Comparison of D-N O-S code simulation with upstream single Langmuir and RFA temperatures.

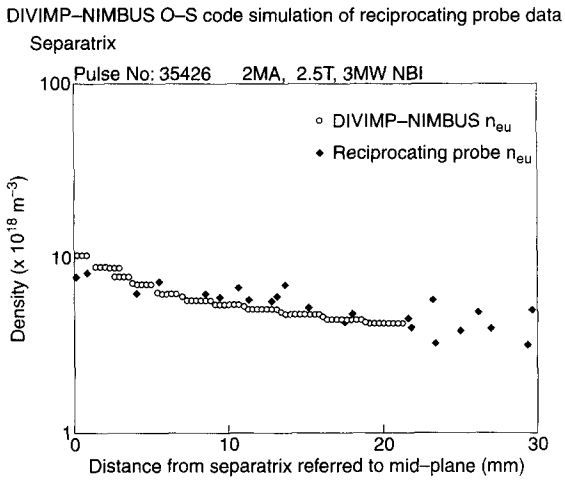

Fig. 6. Comparison of D-N O-S simulation with upstream single Langmuir probe densities.

4.2.2. L-Mode

$I_p = 2$ MA, $B_T = 2.9$ T, $\overline{n_e} = 2.7 \times 10^{19}$ m^{-3},

with ≈ 3 MW of NBI.

D-N O-S code predictions of upstream T_e and T_i across the SOL are compared with single Langmuir and RFA probe results in Fig. 5. Here $T_{it} = T_{et}$ is used as input data for the code, which gives a better fit than choosing a higher T_{it}.

The comparison between code prediction and measured upstream density, from the single Langmuir probe, is shown in Fig. 6. The agreement is good.

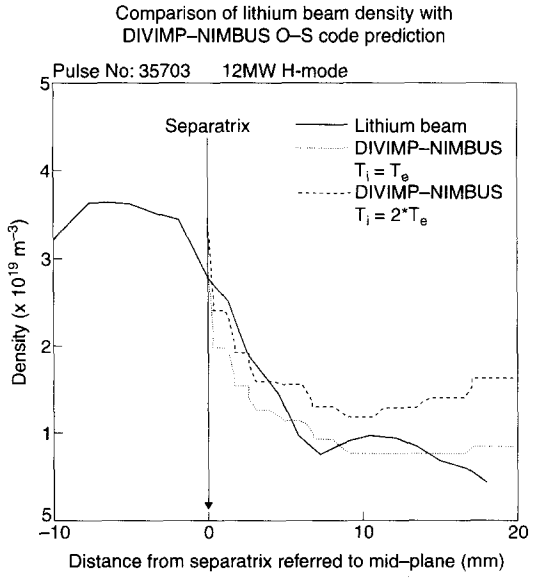

Fig. 7. Code simulation of upstream density measurements taken using a lithium beam.

4.2.3. H-Mode

$I_p = 5$ MA, $B_T = 4$ T, $\overline{n_e} = 7.5 \times 10^{19}$ m^{-3}

with ≈ 12 MW of NBI.

In this simulation the lithium beam diagnostic was used to measure upstream density to inside the separatrix. In this H-mode discharge the volume-average density was increasing and central temperature falling after operation in the hot ion mode. For the simulation, two code runs with $T_{it} = T_{et}$ and $T_{it} = 2T_{et}$ were made. In Fig. 7, the lithium beam results fall between the code simulations, in general, and are well within the experimental errors of the input target data.

5. Discussion

The agreement between D-N O-S code predictions of upstream parameters and upstream experimental measurements is excellent, particularly in view of uncertainties which can arise in the interpretation of probe data, for example the effects of ion Larmor radius on target probe areas. This is not a problem with upstream probes which are large and at normal incidence to the field lines. However, upstream parameters are insensitive to errors in target probe data. For example, assuming a Bohm sheath:

$$(1 - f_t) q_{\parallel} = \gamma n_{et} k T_{et} C_{st} \ (\mathrm{W\ m^{-2}}). \tag{7}$$

where f_t is the fraction of $q_{\parallel}$ radiated in the divertor before reaching the target (assumed to be constant at 0.3 for the discharges studied here), and γ is the sheath transmission factor. If we make the crude global assumption that:

$$q_{\parallel} A_{sol} = (1 - f_s) P_T \ (\mathrm{W}). \tag{8}$$

where f_s is the fraction of the input power, P_T, radiated in the core and $A_{sol} = 4\pi R(B_\theta / B_T)\lambda_{pu}$, where λ_{pu} is the upstream power scrape-off thickness, then using Eqs. (1), (2), (7) and (8) we find:

$$n_{eu} \propto n_{et}^{1/3} \ \mathrm{m^{-3}}. \tag{9}$$

A similar weak dependence may be found for upstream temperature in terms of target temperature. This analysis is crude (T_{et} assumed $\ll T_{eu}$, no radiative or friction losses), yet illustrates the robustness of upstream density against possible experimental errors in measurements of target density. However, where upstream predictions do differ from experimental measurements by a factor 2, this suggests a factor 8 discrepancy in target data which is unlikely. In such cases one would search for a physical reason for the upstream discrepancy.

All predictions in ohmic, L-mode and H-mode are within experimental error, except perhaps for $T_i(r)$ in Fig. 5, which is a factor 2 lower than predicted close to the separatrix. This could be rectified by making $T_{it} \ll T_{et}$

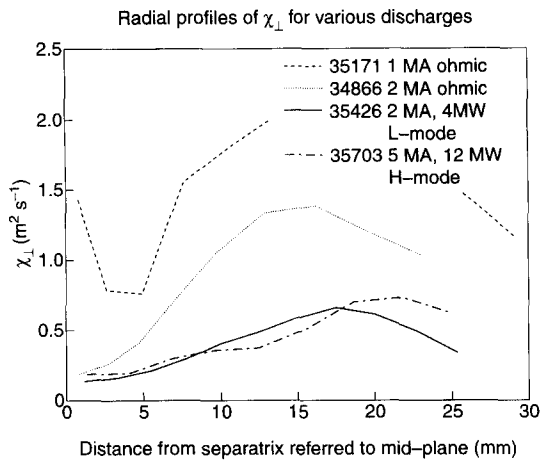

Fig. 8. $\chi_\perp$ extracted from the D-N O-S code solution plotted as a function of radius for various types of discharge.

(which seems unlikely), or by increasing the effect of convection close to the separatrix. This latter possibility was investigated by switching convection off in the code. $T_e(r)$ was almost unaffected (conduction dominates in the electron channel), but $T_i(r)$ *increased* by 5–10%.

5.1. Cross-field heat diffusion coefficient – $\chi_\perp$

The transport coefficient extractor in the DIVIMP code can be used to find χ_{eo} for electrons and χ_{io} for ions in the outer scrape off layer. Here, the average $\chi_\perp$ for both particles, averaged for the inner and outer SOL is extracted as a function of radial location in the SOL, Fig. 8.

Note that these are average values of $\chi_\perp$; χ_{eo} was found to be higher by a factor 2–2.5. Clearly $\chi_\perp$ increases with distance from the separatrix for all types of discharge, a result also found by Shimizu et al. on JT60U [8], and more recently by LaBombard et al. [9]. The $T(r)$ profiles tend to flatten with increasing r, which corresponds to increasing $\chi_\perp(r)$. $\chi_\perp$ does not decrease in H-mode, however, as found previously by Monk et al. on JET [6]. The fall in $\chi_\perp$ beyond the maxima results from target data with low and uncertain J_{sat} far out in the SOL — and may not be realistic.

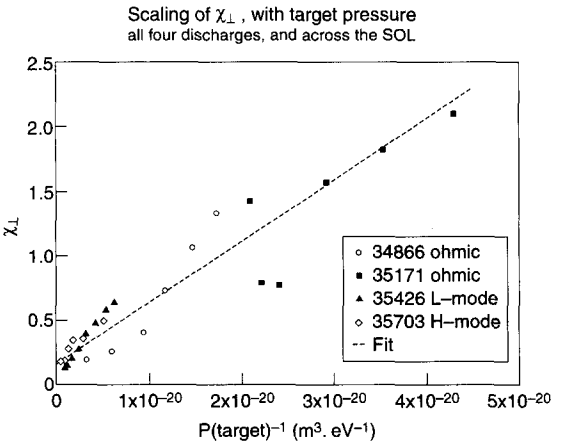

Fig. 9. Scaling of $\chi_\perp$ with target pressure in the SOL, for all discharges.

A scaling of $\chi_\perp$ with pressure (which is conserved in the SOL along field lines) shows a dependence $\chi_\perp \propto P_t^{-1}$, Fig. 9. Since only 4 discharges are included, however, this result may not be indicative of a more general behavior.

6. Conclusions

Using J_{sat} and T_e measurements from target probes in the JET divertor, upstream plasma parameters in the SOL have been predicted using the DIVIMP-NIMBUS 'onion-skin' model for a variety of ohmic, L-mode and H-mode discharges. Good agreement between upstream experimental measurements of T_e (Langmuir probes), T_i (RFA), and n_e (lithium beam) and code predictions are found. The inclusion of convective terms in the code has a small but helpful effect in the prediction of upstream T_i.

$\chi_\perp$ is found to increase with distance from the separatrix in ohmic, L and H mode discharges. A value of $\chi_\perp$ at the separatrix of ≈ 0.3 m^2 s^{-1} is found for most discharges, independent of discharge type and input power.

$\chi_\perp$ is found to scale approximately as $\chi_\perp \propto P_t^{-1}$ throughout the SOL. This result for only 4 discharges may not be indicative of more general behavior.

Having validated the DIVIMP-NIMBUS O-S code with upstream experimental measurements, we are now in a position to produce a more extensive $\chi_\perp$ database using target data alone, which is produced for most discharges. For discharges where volumetric power losses, neutral friction, recombination, etc. is important, the more advanced version of the D-N O-S code [5] will be used.

References

[1] P.C. Stangeby and J.D. Elder, Nucl. Fusion 35 (1995) 1391.
[2] A. Taroni, G. Corrigan, R. Simonini, J. Spence and G. Vlases, Cont. Plasma Phys. 34 (1994) 448.
[3] D. Reiter, J. Nucl. Mater. 196–198 (1992) 80.
[4] E. Cupini, A. De Matteis and R. Simonini, NET Report EUR MI 324/9, CEC Brussels (1984).
[5] P.C. Stangeby, J.D. Elder, W. Fundamenski et al., these Proceedings, p. 358.
[6] R.D. Monk, L.D. Horton, A. Loarte, G.F. Matthews and P.C. Stangeby, J. Nucl. Mater. 220–222 (1995) 612–616.
[7] D.D.R. Summers et al., these Proceedings, p. 391.
[8] K. Shimizu, K. Itami, H. Kuba, N. Asakura and M. Shimada, J. Nucl. Mater. 196–198 (1992) 476–480.
[9] B. LaBombard, J. Goetz, I. Hutchinson et al., these Proceedings, p. 149.